Human Molecular Genetics, 2009, Vol. 18, No. 24 ***4830–4842***
doi:10.1093/hmg/ddp455
Advance Access published on September 29, 2009

Selective neuronal requirement for huntingtin in the developing zebrafish

Tanya L. Henshall, Ben Tucker, Amanda L. Lumsden, Svanhild Nornes, Michael T. Lardelli and Robert I. Richards*

ARC Special Research Centre for the Molecular Genetics of Development and Discipline of Genetics, School of Molecular and Biomedical Sciences, The University of Adelaide, Adelaide, SA 5005, Australia

Received July 14, 2009; Revised September 3, 2009; Accepted September 23, 2009

Huntington's disease shares a common molecular basis with eight other neurodegenerative diseases, expansion of an existing polyglutamine tract. In each case, this repeat tract occurs within otherwise unrelated proteins. These proteins show widespread and overlapping patterns of expression in the brain and yet the diseases are distinguished by neurodegeneration in a specific subset of neurons that are most sensitive to the mutation. It has therefore been proposed that expansion of the polyglutamine region in these genes may result in perturbation of the normal function of the respective proteins, and that this perturbation in some way contributes to the neuronal specificity of these diseases. The normal functions of these proteins have therefore become a focus for investigation as potential pathogenic pathways. We have used synthetic antisense morpholinos to inhibit the translation of huntingtin mRNA during early zebrafish development and have previously reported the effects of huntingtin reduction on iron transport and homeostasis. Here we report an analysis of the effects of huntingtin loss-of-function on the developing nervous system, observing distinct defects in morphology of neuromasts, olfactory placode and branchial arches. The potential common origins of these defects were explored, revealing impaired formation of the anterior-most region of the neural plate as indicated by reduced pre-placodal and telencephalic gene expression with no effect on mid- or hindbrain formation. These investigations demonstrate a specific 'rate-limiting' role for huntingtin in formation of the telencephalon and the pre-placodal region, and differing levels of requirement for huntingtin function in specific nerve cell types.

INTRODUCTION

Huntingtin (htt) is a large 350 kDa protein that while ubiquitously expressed is more abundant in the brain. Expansion of the polyglutamine-coding region in the amino terminus of htt results in a devastating neurodegenerative disease, Huntington's disease (HD). HD is associated with progressive and debilitating motor, cognitive and psychological symptoms (1,2). Presently, there is no treatment or cure for this disease, which is fatal usually 15–20 years after onset.

The primary pathology of HD involves gradual and selective death of medium spiny γ-aminobutyric acid (GABA)-utilizing neurons of the striatum, and neurons in the deeper layers of the cerebral cortex. It is currently not known how the expansion of the polyglutamine-containing region within htt gives rise to this pathology (3,4). The dominant inheritance characteristic of the disease suggests that the polyglutamine expansion may confer a toxic gain-of-function upon htt. Interestingly, the same polyglutamine expansion mechanism is found to be the same basis for eight other neurodegenerative diseases, albeit in eight distinct and unrelated proteins. Each disease shows a distinct neuronal pattern of vulnerability to pathology. These distinctions have been proposed to indicate that the loss or alteration of the unique normal functions of these proteins contribute in some way to the specificity of neuronal cell death (5). In order for this to be the case, different neuronal cell types must therefore have different needs for htt function for their survival. Analysis of the normal role of htt may therefore provide some understanding of the molecular and cellular basis of the pathology associated with HD.

*To whom correspondence should be addressed. Tel: +61 883037541; Fax: +61 883037534; Email: robert.richards@adelaide.edu.au

Since its identification over a decade ago, some insight has been gained into the biological functions of htt. Analysis of its structure and the dozens of binding partners provide clues to htt's function in a variety of processes including cell survival, endocytosis, axonal transport and neuronal transcription (reviewed in 6). Of particular interest is htt's ability to regulate the expression and transport of neurotrophin BDNF, which plays an important role in neuronal survival and differentiation (7–10). Expansion of the polyglutamine repeat region in htt impairs both production and transport of BDNF (8,10,11).

Knock-out of the mouse orthologue, *Hdh*, demonstrated that htt is required for development. Investigation of very early $Hdh^{-/-}$ mouse embryos, prior to embryonic lethality, suggests a role for htt in embryonic organization, patterning, cell survival and nutrient transfer between the embryo and the extra-embryonic tissue (12–17). Limited information can be gained from these $Hdh^{-/-}$ mouse embryos with complete absence of htt due to the early age of lethality and highly disorganized structure of the embryo.

In the current study, we have carried out an investigation of the functions of htt *in vivo*, using an alternative animal model system, *Danio rerio*. We have used morpholino oligonucleotides to inhibit translation of the htt protein from the one cell stage of development. One major advantage of using this system is that we are able to partially reduce the level of htt expression in order to gain a milder phenotype than achieved with $Hdh^{-/-}$ mice. Our previous analysis using this model has demonstrated dramatic effects on embryogenesis upon reduction of htt expression (18). This investigation revealed a role for htt in iron homeostasis and transport in zebrafish (18). Using the same model system, htt was also shown to be required for differentiation of cartilage of the pharyngeal arches, a process which was shown to involve BDNF signaling (19). Here we show that htt plays a role in formation of the anterior most region of the neural plate, specifically in formation of telencephalic progenitor cells and the pre-placodal tissue. Subsequent inhibition of formation of sensory neurons arising from the placodal tissue is rescued by addition of exogenous BDNF.

By using morpholinos to reduce htt levels in the developing zebrafish, we have demonstrated that neuronal cells have differing requirements for htt function. Given that perturbation of normal htt function is a component of HD pathogenesis, this differing requirement of particular neurons for htt function provides a mechanism that can account for the specificity of neuropathology in HD brains despite the widespread expression of htt in the brain.

RESULTS

Htt signaling is required for normal peripheral sensory neuron development in zebrafish

In this study, the zebrafish model system was used to determine the effects of reduced htt expression on early development. The aim of these experiments was to determine whether the normal functions of htt would be rate-limiting for particular developmental processes involving the nervous system and therefore indicate specificity of neuronal requirement for htt function.

Previous studies have suggested that htt may play a role in the prevention of apoptosis (20). We therefore decided to look at the general pattern of apoptosis within the whole embryo at various stages of development, after injection of a morpholino targeted to the zebrafish *htt* mRNA at the one cell stage. This validated zebrafish model of htt function has been previously described by our laboratory (18) and has also recently been utilized by others (19,21).

Acridine orange was used to view cell death throughout development in the whole *hd*MO1 embryo. As cell death is a normal part of development, the pattern of cell death in *hd*MO1 embryos was compared with that of two control groups, wild-type (uninjected) and *c*MO injected embryos. Very similar results were obtained for wild-type and control morpholino injected embryos (*c*MO or *mc*MO1) in all experiments in this manuscript. For simplicity, only one control group image is shown, and as injection of a control morpholino is a more stringent test of morpholino specificity, these images are shown.

When analyzing the level of apoptosis with acridine orange, of particular note was the reduction in cell death within the olfactory placode (Fig. 1A and B) and within the lateral line neuromasts (result appears similar to Fig. 1E and F described below) of *hd*MO1 embryos (Fig. 1B and F) compared with either of the control groups (Fig. 1A and E). Cell death is a normal and continuous process within both the olfactory and lateral line sensory systems to allow constant replenishing of sensory neurons from the basal support cell population (22–24). The absence of cell death in these regions suggests either that these sensory neurons are not able to undergo cell death in *hd*MO1 embryos, or that these sensory neurons are not present with the olfactory or lateral line placodes. In order to further investigate this phenotype, two dyes were used which are specifically taken up by olfactory sensory neurons and lateral line neuromasts. DiI is a lipophillic dye used previously to visualize mature olfactory sensory neurons in zebrafish (25). Staining embryos in this dye revealed an absence of mature olfactory sensory neurons in the olfactory placode of *hd*MO1 embryos at 96 hpf (Fig. 1D) unlike the control (*mc*MO1) injected embryos (Fig. 1C). Similarly, quantitative PCR (qPCR) analysis of olfactory marker protein 2 (*zOMP*), expressed by mature olfactory sensory neurons (26), is significantly reduced in *hd*MO1 embryos compared with *mc*MO1 embryos (Table 1).

Like DiI, DASPEI staining is used to visualize sensory neurons; however, DASPEI is specifically taken up by hair cells within the lateral line neuromasts (27). In the wild-type embryo, the number and pattern of lateral line neuromasts is well characterized (28). DASPEI staining showed that *hd*MO1 embryos have fewer lateral line neuromasts compared with wild-type and *mc*MO1 injected embryos (Fig. 1E and F). Quantification of the total number of neuromasts in each embryo shows that this reduction occurs as a dose-dependent response to *hd*MO1 injection (Fig. 1G).

Htt has a rate-limiting role in anterior neural plate formation

Both the olfactory and lateral line sensory systems arise from specialized regions of embryonic ectoderm termed the

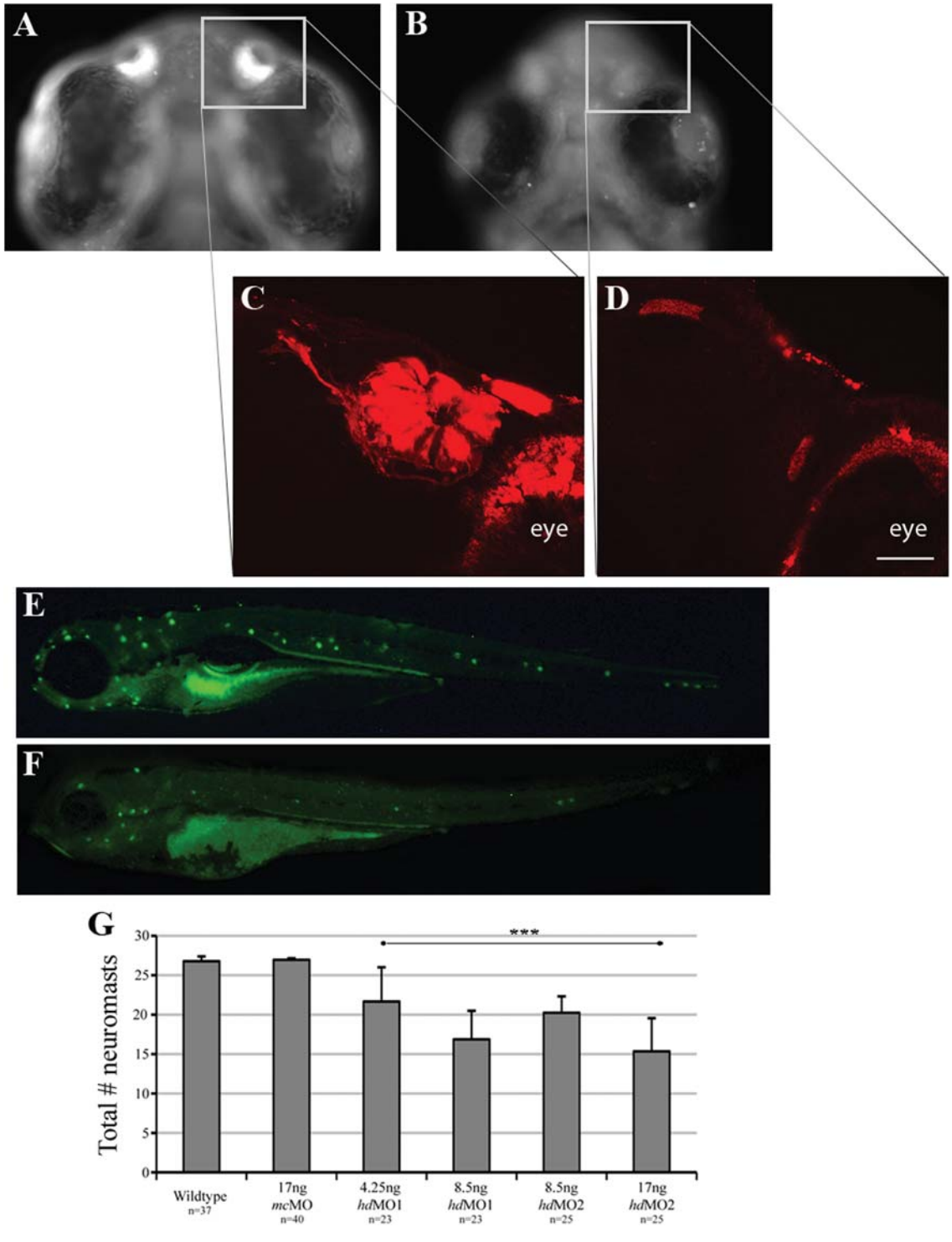

Figure 1. Htt is required for development of the olfactory and lateral line sensory systems of zebrafish. (**A** and **B**) *hd*MO1 embryos show reduced level of apoptosis in the olfactory placode visualized by staining with acridine orange. (**C** and **D**) Mature olfactory sensory neurons are absent in olfactory placode of *hd*MO1 embryos unlike in *c*MO embryos as revealed by staining with DiI. (**E** and **F**) DASPEI staining revealed *hd*MO1 embryos have a reduced number of lateral line neuromasts compared with wt or *mc*MO1 embryos. (**G**) Reduction of htt expression significantly affects the number of neuromasts in a dose dependent manner. ***Significance is determined by *P*-value = <0.001. *P*-values were determined by a Student's *t*-test comparison of each group to wt. Wt versus *mc*MO1 comparison showed no evidence of a significant effect due to *mc*MO1 injection. *P*-values = 17 ng *mc*MO1, 0.10637499; 4.25 ng *hd*MO1, 1.83991E−08; 8.5 ng *hd*MO1 5.16023E−21; 8.5 ng *hd*MO2, 2.82275E−23; 17 ng *hd*MO2, 5.56472E−21. (A–D) 8.5 ng of morpholino injected per embryo; (E and F) 17 ng *hd*MO1 injected per embryo. (A–D) Ventral views of embryos at 72 hpf. (E and F) Lateral views of embryos at 96 hpf, anterior to the left. Numbers of embryos displaying the described phenotypes were (A and B) *c*MO1 0/53, *hd*MO1 26/37. Representative embryos shown; (A, C and E) *c*MO1 injected embryos, (B, D and F) *hd*MO1 injected embryos. Scale bar = 25 μm.

Table 1. Quantitative PCR analysis of various genes within the neural plate and derivative tissue, the olfactory receptor neurons

Plot order	Gene	Treat	Estimate	Log10-Fold change	SE	T-Stat	DF	Adjusted *P*-value	Significance
hdMo1 versus mcMo1									
1	*dlx3b*	hdMo1 versus mcMo1	−1.17221	−14.867	0.1684	−6.959	66	8.94E−09	***
2	*emx3*	hdMo1 versus mcMo1	−1.20867	−16.169	0.1257	−9.613	53	4.60E−12	***
3	*ntl*	hdMo1 versus mcMo1	−0.00583	−1.014	0.0610	−0.096	80	0.9238	
4	*zOMP*	hdMo1 versus mcMo1	−0.30378	−2.013	0.1105	−2.749	47	2.96E−02	***
5	*otx2*	hdMo1 versus mcMo1	−0.25161	−1.785	0.1213	−2.075	50	0.1007	
6	*six1*	hdMo1 versus mcMo1	−1.07600	−11.912	0.1437	−7.491	53	5.12E−09	***
7	*val*	hdMo1 versus mcMo1	−0.15320	−1.423	0.0736	−2.081	51	0.1007	
wt versus mcMo1									
1	*dlx3b*	wt versus mcMo1	−0.19321	−1.560	0.1667	−1.159	66	0.3900	
2	*emx3*	wt versus mcMo1	−0.12011	−1.319	0.1257	−0.955	53	0.4815	
3	*ntl*	wt versus mcMo1	0.11289	1.297	0.0604	1.870	80	0.1303	
4	*zOMP*	wt versus mcMo1	−0.13956	−1.379	0.1105	−1.263	47	0.3724	
5	*otx2*	wt versus mcMo1	−0.04433	−1.107	0.1193	−0.372	50	0.8153	
6	*six1*	wt versus mcMo1	0.04467	1.108	0.1437	0.311	53	0.8153	
7	*val*	wt versus mcMo1	−0.02317	−1.055	0.0723	−0.320	51	0.8153	

'Estimate' column shows raw values representing arbitrary units of RNA transcript as determined by the standard curve showing expression of each gene relative to expression of the control gene, *elongation factor* (*ef-1a*) (78). *** Significance is determined by *P*-value ≤ 0.001. For *hd*MO1 versus *mc*MO1, *dlx3b, emx3, zOMP* and *six1* all show statistically significant evidence of differential regulation with $P \leq 0.001$. *ntl, otx2* and *val* do not show statistically significant evidence of differential regulation. None of the wt versus *mc*MO1 comparisons show any evidence of a significant effect due to *mc*MO1 injection. 8.5 ng of morpholino injected per embryo. All embryos were analysed at 12 hpf except *zOMP* which was analysed at 48 hpf. Abbreviations: DF, degrees of freedom; se, standard error.

olfactory and lateral line placode, respectively. These are among a number of placodal tissues that originate from a common precursor region, the pre-placodal region, early in gastrulation of all vertebrates (reviewed in 29–34). Given this common origin, we speculate that htt may be important in formation of the pre-placodal region. *Six1*, orthologue of *Drosophila sine oculis*, encodes a homeodomain transcription factor expressed throughout the pre-placodal region and in all cranial placodes throughout development (35). We analysed the mRNA expression pattern of *six1* at 12 hpf in an attempt to visualize the pre-placodal region in the developing zebrafish. *In situ* hybridization analysis revealed a clear reduction in the level of *six1* expression in the pre-placodal region of *hd*MO1 embryos (Fig. 2A and B). At this time in normal development, placodal cells have formed at the anterior end of the neural plate and some of the placodal cells (the lateral line and otic placodes) have broken away and are migrating posteriorly toward their final destination. *Six1* expression appears to be reduced in both areas in *hd*MO1 embryos (Fig. 2B). Quantitation of the overall level of *six1* mRNA expression by qPCR analysis shows that *six1* expression was significantly reduced in *hd*MO1 zebrafish embryos (Table 1). In support of this result, expression of a second marker of pre-placodal cells which are more specifically expressed within the olfactory precursor cells, *Drosophila distal-less* orthologue, *dlx3b* was also shown to be significantly reduced in *hd*MO1 embryos (Table 1) (36). This reduction in *six1* and *dlx3b* expression suggests that htt has a rate-limiting role during development in the formation of the pre-placodal region.

Fate and expression mapping (36–39) has been carried out for cells of the zebrafish anterior neural plate. Figure 2C demonstrates the position of pre-placodal tissue expressing *six1* and *dlx3b* at the anterior ridge of the neural plate. Immediately adjacent to this, telencephalic precursor cells at the neural plate margin express *emx3* (green) (40–42). qPCR analysis of *hd*MO1 embryos revealed reduced expression levels of *emx3* (Table 1) suggesting that htt is also required for formation of neural-fated ectoderm, not only the pre-placodal region. This result correlates with reduced expression of *dlx2* within the subpallial telencephalon and diencephalon later in the development (Fig. 2D and E). Interestingly, anterior neural plate expression of *otx2* (slightly more posterior to *emx3*) was not significantly reduced in *hd*MO1 embryos by qPCR (Table 1) and *in situ* hybridization analysis, with no change in the pattern of expression (Fig. 2F and G).

In an effort to identify the cellular location and developmental process(es) in the neural plate for which htt activity was rate-limiting, we examined the expression of a number of genes, which are markers for known regions of the neural plate, neural plate derivative tissues and also for notochord formation. First, we selected genes that are expressed at specific locations along the neural plate from the forebrain to the hindbrain. As visualized by *in situ* hybridization, expression of *krox20* and *hoxd4a* genes within the hindbrain (expressed in rhombomere 3 and 5, and rhombomere 7+, respectively) were not altered in *hd*MO1 embryos (Fig. 3A and B). In addition, expression of neural crest cell marker *dlx2* at 19 hpf demonstrated that in *hd*MO1 embryos, cranial neural crest cells form in the same three-group pattern in the hindbrain as seen in both *mc*MO1 and wild-type embryos (Fig. 3C and D).

In 2005, Woda *et al*. (15) showed that $Hdh^{-/-}$ mouse embryos at e6.5 had reduced neuroectoderm formation, and lack a morphological node. This was suggested to be caused by a deficiency in formation of the anterior primitive streak (anterior blastopore; anterior blastoderm margin in zebrafish (43)). The blastoderm margin is required for the formation of the germ layers. To investigate whether a deficiency in the anterior blastoderm margin gives rise to the anterior neural plate deficiency phenotype observed here, we examined mesoderm formation in *hd*MO1 embryos. *In situ* hybridization

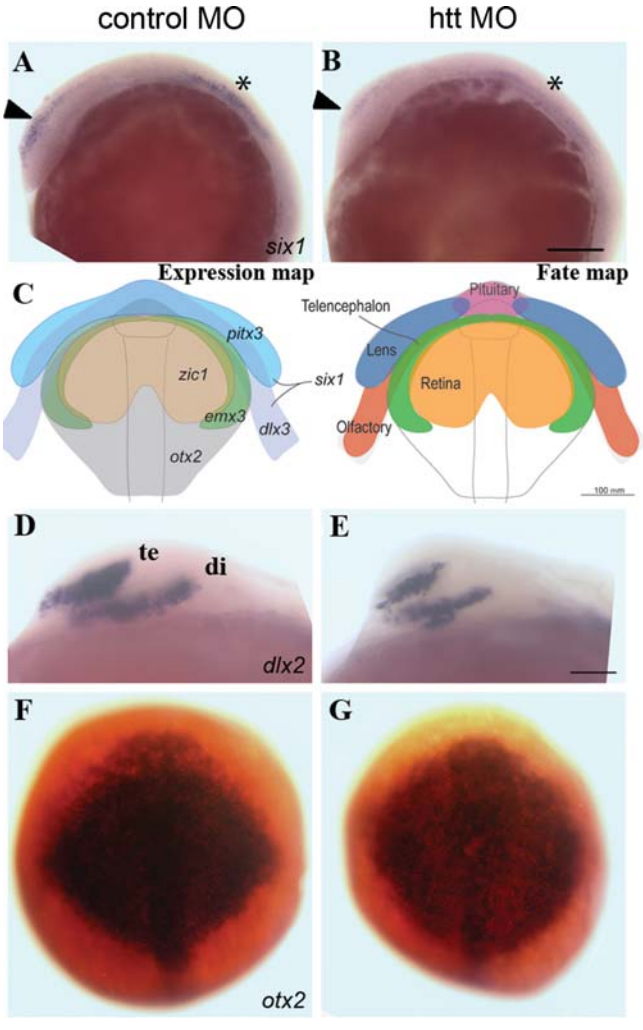

Figure 2. RNA *in situ* hybridization and qPCR reveal htt is required specifically for the formation of the anterior neural plate. (**A** and **B**) *hd*MO1 embryos show reduced expression of *six1* in the pre-placodal region (arrow head) compared with *mc*MO1 embryos. Asterisk shows lateral line and otic placode cells migrating toward the posterior in (A) which are also reduced in *hd*MO1 embryos (B). (**C**) Schematic drawings showing expression and fate maps of the zebrafish anterior neural plate and pre-placodal field at the end of gastrulation (32,36,39). The location of particular cell fates in the anterior neural plate and pre-placodal field correlate to gene expression patterns. All placodal tissues express *six1* (32), and in addition express one (or a number of) other genes as listed; adenohypophysis precursor cells (pituitary) express *dlx3b* and *pitx3*. Lens precursors express *pitx3* or *pitx3* and *dlx3b*. Olfactory precursors express *dlx3b* and *pitx3*, or only *dlx3b*. Anterior neural plate tissues, which are not derived from the pre-placodal region include: telencephalic precursor cells (expressing *emx3*, or *emx3* and *zic1*) and retinal precursors (expressing *zic1*). The *otx2* expression domain in the anterior neural plate is shown in grey. Dorsal view, anterior to top. (**D** and **E**) At 19 hpf, *hd*MO1 embryos have reduced expression of *dlx2*, particularly in the subpallial telencephalon (te), but also in the diencephalon (di). Expression of anterior neural plate marker *otx2* is only slightly reduced in *hd*MO1 embryos by *in situ* hybridization (**F** and **G**). (A and B) 20 hpf, (D and E) 19 hpf, (F and G) 10 hpf. (A, B, D and E) Lateral view, anterior to the left, (F, G) dorsal view, anterior to the top. Numbers of embryos displaying the described phenotypes were (A and B) wt, 7/22, *mc*MO1 3/45, 8.5 ng *hd*MO1 25/46, 17 ng *hd*MO1 34/40, results combined from two independent experiments; and (D and E) wt, 0/12, *mc*MO1 1/18, 17 ng *hd*MO1 15/18. Representative embryos shown. Abbreviations: te, telencephalic *dlx2* streak; di, diencephalic *dlx2* streak. Scale bars represent (A, B) 200 μm and (D, E) 100 μm.

of mesodermal marker, *no tail (ntl)* in *hd*MO1 embryos showed no change in pattern of expression in the notochord compared to control embryos, however lower expression within the tailbud was observed (Fig. 3E–H and Table 1) (44). The tailbud is important for the formation of posterior structures of the developing embryo, both axial and non-axial structures such as the notochord and the tail, respectively (45,46). With high doses of morpholino, *hd*MO1 embryos appear to have a curled tail (18) which suggests deficiency in the non-axial mesoderm. Importantly, within the tail bud, *hd*MO1 embryos still form the Kupffer's vesicle, the zebrafish structure equivalent to the mouse node and required for left–right patterning (47). These investigations demonstrate that *hd*MO1 embryos are deficient only in the very anterior margin of the neural plate and suggest a possible role for htt in the formation of this region. Appropriate formation of the notochord suggests that this is not due to deficiency in the anterior blastoderm margin. These results also show that htt does not play a rate-limiting role in the formation of the midbrain or hindbrain, or in anterior–posterior patterning of the neural plate at this reduced level of htt expression.

To further elucidate the mechanism of anterior ectoderm deficiency in *hd*MO1 embryos, investigation into embryonic tissues required for formation of this region was carried out. In zebrafish, the yolk syncytial layer (YSL) plays an important role in the formation of the anterior neuroectoderm in a similar manner to the anterior visceral endoderm in mouse (48). At 30% epiboly (4.7 hpf), *sox32* is expressed by cells of the YSL and presumptive endoderm. By *in situ* hybridization analysis, there appears to be no change in the abundance or pattern of cells in the YSL in *hd*MO1 embryos (Fig. 3L) compared with the control embryos (Fig. 3I). This suggests that the reduction in htt levels to this experimental level does not alter the formation of the YSL and therefore that this is not a cause of the reduction in anterior ectoderm derivatives seen in *hd*MO1.

Like the node in mouse and chick, the zebrafish shield has an essential role in the induction of anterior neural tissue (reviewed in 49). We analyzed the expression of the gene, *goosecoid* (*gsc*), that is normally expressed within the zebrafish organizer at shield stage (6 hpf) and plays an essential role in dorso-ventral patterning and formation of forebrain development (50). We found that injection of *hd*MO1 did not affect the pattern or level of *gsc* expression in the organizer (Fig. 3M and N) suggesting that perturbation in organizer activity does not play a role in the *hd*MO1 phenotype described herein.

Htt is important for neural crest cell differentiation into cartilage

Gross analysis of the morphology of *hd*MO1 embryos revealed disruption in tissues of the mouth. This was especially evident after staining with acridine orange (Fig. 1A and B) with no increase in cell death seen in this region. However, the acridine orange staining provided some contrast within the transparent embryo, exposing the external pharyngeal morphology. As the structure of the branchial region lies over the cartilage

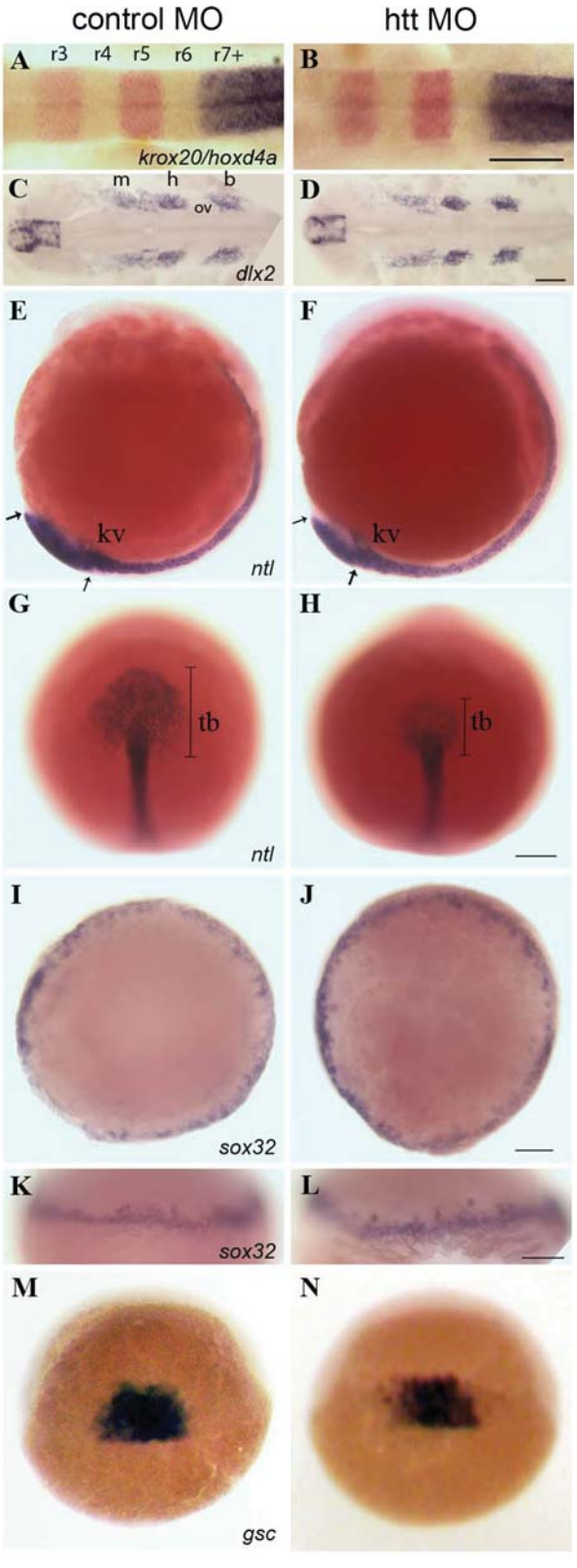

Figure 3. Further characterization of the *hd* MO1 neural plate phenotype. (**A**–**D**) Reduction in Htt expression does not alter anterior–posterior brain patterning. (A and B) *In situ* hybridization analyses of *krox-20* (red) and *hoxd4a* (purple) show the segmental nature of the zebrafish hindbrain into rhombomeres. The hindbrain of *hd*MO1 (B) is unaltered when compared with *c*MO1 (A). (C and D) *In situ* hybridization of *dlx2* shows that neural crest cells arise at the lateral edge of the neural plate in the correct pattern. Htt does not affect formation of the notochord, however *hd*MO1 embryos (**F**) have a noticeably smaller tailbud compared with *c*MO1 embryos (**E**; compare distance between arrows in each image. Also compare length of bars in dorsal view; **G**, **H**). (**I** and **J**) The YSL of *hd*MO1embryos is indistinguishable from that of *mc*MO1 embryos by *in situ* hybridization of *sox32*. (**M** and **N**) Reduction in htt expression does not alter formation of the node shown here by expression of *gsc*. (A–D) Dorsal views of embryos at 19 hpf, anterior to the left; (E and F) lateral views of embryos at 12 hpf, anterior to the left; (G and H) dorsal views of embryos at 12 hpf; (I and J) dorsal views of embryos at 30% epiboly; (K and L) lateral views of embryos at 30% epiboly, dorsal to the top; (M and N) lateral views of embryos at 60% epiboly, dorsal to the top. Numbers of embryos displaying the described phenotypes were (G and H) *c*MO1 8/47, *hd*MO1 27/35. Representative embryos shown. Abbreviations: r3-r7+, rhombomere 3 to rhombomere 7 onward; ov, otic vesicle; m, mandibular group; h, hyoid group; b, basihyal group; kv, kupffler's vesicle; tb, tailbud; cnc, cranial neural crest. All scale bars represent 200 μm. All embryos in left column except (A) and (C) have been injected with *mc*MO1, (A) and (C) are *c*MO embryos. All embryos in right hand column are *hd*MO1 embryos. All embryos were injected with 17 ng of morpholino, except (C) and (D) injected with 8.5 ng morpholino.

skeleton, it seemed likely that *hd*MO1 embryos would have an altered cranioskeletal structure. Alcian blue was used to stain the cartilage of *hd*MO1 embryos in order to visualize this disruption (Fig. 4A–C). At a moderate dose of morpholino (8.5 ng), *hd*MO1 embryos (Fig. 4B) have fully formed pharyngeal arch 1 (p1; or Meckel's cartilage) and p2 (or ceratohyal) cartilages. In 25% of embryos, the p2 is pointing in a caudal rather than rostral direction. An example of this is shown in Figure 4B. Approximately 70% of all *hd*MO1 embryos show partial or complete loss of p3–p7 cartilages. During preparation of this manuscript, a similar phenotype was described using this model (19).

In an effort to investigate further, the cause of this phenotype, *in situ* hybridization analysis of *dlx2* expression was used to visualize the undifferentiated cartilage forming cells, the cranial neural crest, throughout their development. As shown earlier, the cranial neural crest cells form in the hindbrain in the correct pattern (Fig. 3B), then by 33 hpf they have migrated from the hindbrain into the pharyngeal arches in *hd*MO1 embryos in a similar manner to *c*MO1 embryos (Fig. 4D and E). The arches, containing neural crest cells, are separated from each other by pharyngeal endoderm (non-staining tissue between the arches). At this time, arches p1–p6 are divided by the endoderm, but p6 and p7 have not yet been divided, as seen in Fig. 4D. However, in *hd*MO1 embryos, arches p5–p6 have not yet finished dividing (Fig. 4E, arrow) suggesting a slight developmental delay of craniofacial formation.

In wild-type embryos, the pharyngeal neural crest cells continue to express *dlx2* until they differentiate into cartilage. The process of differentiation begins at approximately 48 hpf. *In situ* hybridization of *dlx2* shows that at 56 hpf, well after onset of differentiation, some *dlx2* is still expressed by neural crest cells of *c*MO embryos (Fig. 4F and G). *dlx2* is also expressed by neural crest cells of *hd*MO1 embryos. This demonstrates that in *hd*MO1 embryos, cartilage precursors have survived beyond the onset of differentiation and it is therefore unlikely that the pharyngeal disruption in *hd*MO1 embryos is due to early apoptosis of pharyngeal neural crest cells. It is

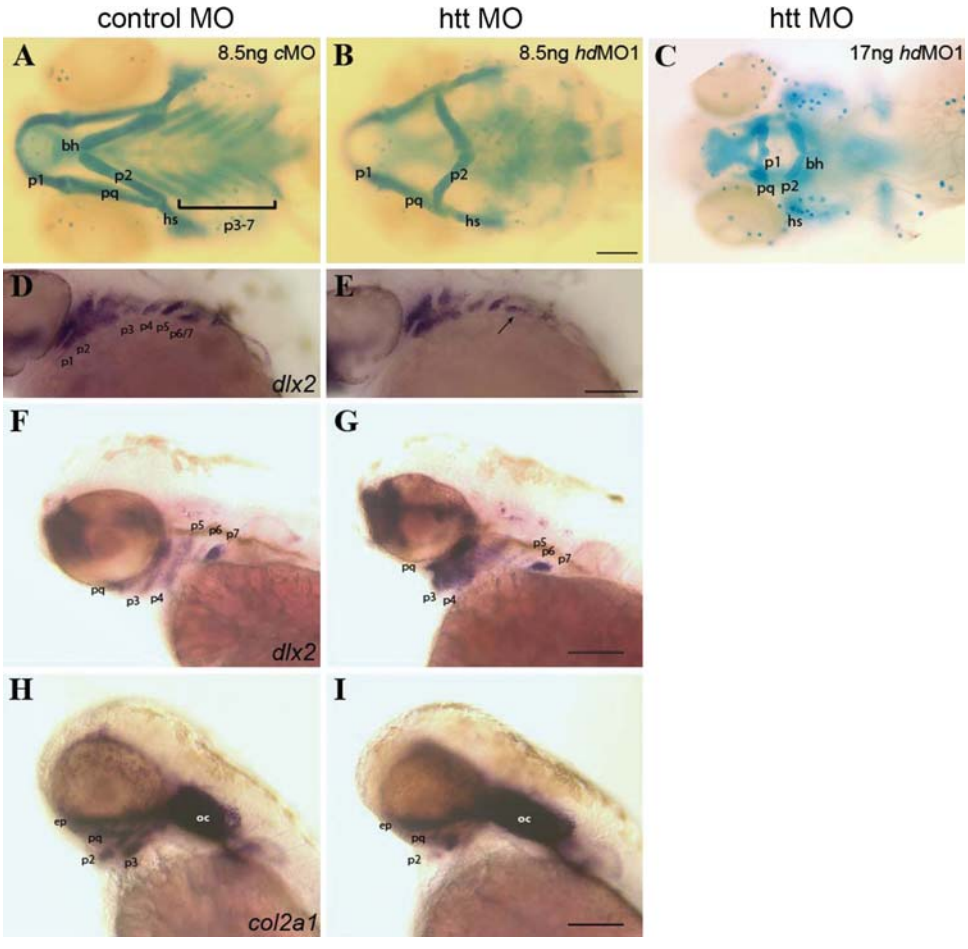

Figure 4. Htt has a role in differentiation of neural crest cells into pharyngeal cartilage. (**A**) Alcian blue shows the normal pattern of cartilage in the pharyngeal region of *c*MO1 embryos. *hd*MO1 embryos have a disrupted craniofacial cartilage structure. (**B**) Some, more severe *hd*MO1 embryos show a malformed p2 (ceratohyal) cartilage, which is pointing in a caudal rather than rostral direction. (**C**) Injection of a higher concentration of *hd*MO1 results in a more severe phenotype; however, p1 and p2 are still present. (**D**–**G**) *In situ* hybridization of *dlx2*, shows undifferentiated cartilage precursor cells are present within the pharyngeal arch endoderm of *c*MO and *hd*MO1-injected embryos at 33 hpf (D and E) and at 56 hpf (F and G), well after onset of neural crest differentiation into pharyngeal cartilage. The reduced level of *col2a1* expression within some cartilage elements, however, suggests that the reduction in htt expression inhibits differentiation of pharyngeal arch cartilage (H and I). (A–C) 7 hpf, (D and E) 33 hpf (20 somites), (F–I) 56 hpf. All scale bars represent 200 μm except (D and E) which equals 100 μm. (A–C) Ventral view, anterior to left. (D–I) Lateral views, anterior to the left. 8.5 ng morpholino injected per embryo, except in (C) where 17 ng morpholino was injected. Representative embryos shown. Numbers of embryos displaying the described phenotypes were: (A and B) 0/33 wt, 1/51 *c*MO, 40/47 *hd*MO1; (H and I) 0/17 *c*MO, 11/12 *hd*MO1. Abbreviations: bh, basihyal; hs, hyosymplectic; p, pharyngeal arch; p3–p7, pharyngeal arch 3–7; pq, palatoquadrate.

possible, however, that reduced htt expression impairs differentiation of neural crest into cartilage.

To investigate the differentiation of pharyngeal cartilage, we analyzed the expression pattern of *col2a1*, a gene expressed by and required for neural crest cells during differentiation into cartilage. At 56 hpf, the most anterior pharyngeal cartilage is differentiating in *c*MO1 embryos including the epiphyseal plate (ep), palatoquadrate (pq), p2 and p3 cartilages (Fig. 3G and H). Differentiation has also begun in *hd*MO1 embryos; however, *col2a1* is reduced in the pq and p2 cartilages, and absent in p3. This result suggests that the absence of many or all of the ceratobranchial cartilage elements is likely to be due to impaired differentiation of these cartilage elements in *hd*MO1 embryos. Injection of a higher dose of *hd*MO1 morpholino still does not affect differentiation of the p1 or p2 cartilage, suggesting that htt at this low level is not a rate-limiting step in p1 and p2 cartilage differentiation, although they are grossly malformed. Initially, it was thought that the caudal pointing p2 cartilage in Figure 4B was due to fusion of this bone to the basihyal (bh) or p3 during development. However, the caudal pointing p1 and p2 cartilages in Figure 4C suggests the cause of this malformation may be lack of development of the underlying endoderm.

BDNF rescues the *hd*MO1 peripheral sensory neuron phenotype

Growth factor, BDNF has been shown previously to play a major role in neural development including formation, survival and differentiation of neurons. htt has been shown to regulate the production and transport of BDNF (7–10) and recently, Diekmann *et al*. (19) showed that exogenous BDNF is able to rescue partially a craniofacial phenotype (in *hd*MO1 embryos) similar to that described earlier. It was

therefore hypothesized that altered BDNF may contribute to the *hd*MO1 sensory neuron phenotypes described in this paper. The number of lateral line neuromasts in zebrafish embryos is well characterized and highly consistent (28). We used DASPEI staining of lateral line neuromasts to determine whether adding BDNF to the embryo medium during development was able to rescue the reduction in neuromast number seen in *hd*MO1 embryos. Exogenous BDNF protein was added to the embryo medium immediately following *hd*MO1 injection. Embryos were allowed to develop in embryo medium with or without BDNF until 120 hpf. Similar to the results shown in Figure 1G, *hd*MO1 embryos had a reduced number of neuromasts than wild-type embryos at 120 hpf, $P = <0.001$ (average neuromast numbers were WT, 26.83 ± 0.38, $n = 42$; *hd*MO1, 20.53 ± 3.75, $n = 49$). BDNF was able to restore partially the number of lateral line neuromasts, shown by a shift in the mean number of lateral line neuromasts toward WT levels (*hd*MO1 versus *hd*MO1+BDNF $P = <0.005$; average neuromast number was *hd*MO1+BDNF, 22.73 ± 2.95, $n = 45$). This result showed a partial but statistically significant rescue of the number of lateral line neuromasts toward wild-type levels, supporting that BDNF plays a role in the sensory neuron phenotype in *hdMO1* embryos. Currently, it is not known at which stage BDNF may play a role in the sensory neuron phenotype caused by reduced htt levels. However, this result highlights the important role of BDNF in htt signaling and development.

DISCUSSION

Htt is a large 350 kDa protein that is ubiquitously expressed throughout development. Expansion of a polyglutamine repeat region in the amino terminus of htt is responsible for the devastating neurodegenerative condition, HD. Although it is widely accepted that the presence of the polyglutamine repeat beyond a threshold number imparts a toxic gain-of-function property to this protein, there is some compelling evidence to suggest that a loss of the normal function of htt contributes to HD pathology, especially its neuronal specificity (reviewed in 6).

Presently, the normal functions of htt are unclear. The many binding partners and biological processes described to date suggest that the cellular functions of htt are numerous, including transcriptional regulation, vesicle trafficking, iron homeostasis and cell survival (reviewed in 6). It has been unclear which, if any, of these functions might be rate-limiting in neurons and therefore candidates for perturbation in HD.

Animal model systems are useful to identify the functions of htt in the complex developing organism. Previously, analysis of htt functions in the mouse model has been difficult due to the early embryonic lethality of homozygous knockout animals and the apparent lack of phenotype in heterozygous animals (12,16,17). Embryonic lethality in these embryos demonstrates that htt plays a critical role in early embryonic development; however, it also makes analysis of the consequences of htt knockout in older embryos difficult.

In the present work, we describe the effects of morpholino-induced inhibition of htt translation in zebrafish embryos. Morpholinos are short strands of non-degradable, synthetic antisense oligonucleotides injected at the one cell stage to block the translation of *htt* mRNA into protein. The benefit of this approach is that the extent of inhibition of htt expression can be varied as can the resulting phenotype by adjusting the dosage of morpholino injected. We have described the use of this model system previously (18) and have used a moderate level of morpholino so as to investigate the effects of a partial reduction of htt expression. With partial htt reduction, *hd*MO1 embryos have impaired formation of the anterior region of the early neural plate as evidenced by reduced expression of genes characteristically present within the pre-placode and anterior neural plate including: *six1*, *dlx3b* and *emx3*. The reduction in anterior neural plate precursor cells later results in a dose-dependent reduction in the number of lateral line neuromasts and also reduction in olfactory sensory neurons and forebrain regions such as the subpallium and diencephalon.

Placodal tissue is a homogeneous layer of embryonic ectoderm that becomes specified early in development to form a number of different tissues. The olfactory and lateral line systems are among a number of placodal tissues that originate from this common precursor region, others include adenohypophyseal, trigeminal, profundal, lens, otic and a series of epibranchial and hypobranchial placodes. It is hypothesized that reduction of the pre-placodal domain will affect all tissues derived from these placodes; including the anterior lobe of the pituitary gland, ganglia of the trigeminal and profundal nerves, lens, otic vesicle and the sensory neurons of the distal ganglia of the face, respectively (32). The downstream effects of disruption in placode formation alone are wide ranging and, in addition to the loss of telencephalic precursor cells, have devastating consequences on embryo development.

While a significant reduction was observed in the level of anterior gene expression (for *six1*, *dlx3b* and *emx3)*, no significant change was observed in the slightly more posterior marker *otx2*. There was also no significant change in markers of mid- and hindbrain tissue (*valentino*, *krox20* and *hoxd4a*), or the hindbrain-derived tissue, the cranial neural crest (*dlx2b*). It therefore appears that the consequences of htt deficiency in *hd*MO1 embryos are restricted to the most anterior regions of the neural plate and pre-placodal region, and do not affect anteroposterior patterning of the neural plate.

The anterior neural plate, along with the cranial dorsolateral endomesoderm, is important for the induction of the pre-placodal region (51). Given this, it is possible that the reduction in pre-placodal tissue occurs as a result of deficiency in the anterior neural plate *emx3* expressing cells, located at the anterior neural plate border region. Therefore, we hypothesize that htt is specifically required for the formation or survival or the anterior neural plate margin, including *emx3* expressing telencephalic precursor cells.

Investigation of the possible cause of anterior neural plate deficiency showed no change in two structures known to be important in the formation of the anterior neural plate, the shield (expressing *gsc*) and the YSL (expressing *sox32*). This result is in contrast to that observed by White *et al*. (14), and Woda *et al*. (15), where $Hdh^{-/-}$ mice did not form a morphological node. The difference between *hd*MO1 and $Hdh^{-/-}$ mice is likely to be due to the small amount of

htt present in *hd*MO1 embryos as a result of the incomplete reduction of htt translation by *hd*MO1, and pre-injection translation of maternally deposited *htt* mRNA in 1-cell *hd*MO1 embryos (18). This small level of htt expression is likely to be sufficient to allow formation of the node in *hd*MO1 embryos and supports that the anterior deficiency is not a result of perturbation in node formation.

During the preparation of this manuscript, another description of brain morphology and apoptosis in zebrafish with reduced htt expression was published (19). In this paper, it was stated that their *hd*MO1 embryos had similar brain morphology to that described earlier in our lab (18). Diekmann *et al*. (19) noted apoptosis within the midbrain and hindbrain of their *hd*MO1 embryos. Our analysis did not reveal the same pattern in apoptosis within the midbrain or hindbrain at anytime during development. However, we observed a significant increase in apoptosis within the optic tectum at 36–48 hpf (data not shown). This result may complement another observation of Diekmann *et al*. (19), showing significantly reduced axonal innervation of this region by retinal axons. At approximately 36–48 hpf, retinal axons are required to make contact with the optic tectum. Any neurons in the optic tectum that are not contacted by retinal axons undergo apoptosis (22). Although retinal precursors form within the anterior region of the neural plate, the anterior neural plate deficiency in *hd*MO1 embryos is not necessarily the cause of this retinal axon phenotype. Retinal precursor cells express *zic1*. This gene is expressed largely within the *otx2*-expressing domain as shown in Figure 2C. As *hd*MO1 embryos do not appear to be deficient in the *otx2* expressing cells, it is unlikely that this phenotype is due to reduction of retinal precursor cell number. It is possible, however, that htt may play a role in retinal development after retinal cell formation, such as in survival, differentiation or axon guidance of the retinal cells. This possibility is supported by a *Drosophila* htt knockout model in which absence of htt leads to retinal degeneration in adult flies (52). The observed neurodegeneration is similar to that caused by overexpression of htt with an expanded polyglutamine region (52). Retinal degeneration is also seen in HD transgenic mouse model R6/2 (53,54) and a human HD patient compared with age-matched control, although only one HD patient was studied (55). This evidence suggests a role for htt in survival of retinal cells, and for perturbation of htt function in the pathogenesis of HD.

Clinical observations of HD patients also reveal some evidence of olfactory impairment. HD patients have been shown to have impaired olfactory detection (56–58), olfactory memory (56,57,59), identification (57,58,60,61) and discrimination of quality and intensity of odors (58). This dysfunction may occur by either of two mechanisms. First, neurodegeneration within brain regions which are important for processing olfactory information is likely to be the cause of impaired olfactory memory, identification and discrimination (59), while impaired odor detection is likely to be due to dysfunction of olfactory neurons. Because of htt's role in anterior neural plate formation shown here, it is possible that either of these mechanisms results from perturbation of normal htt function. These findings therefore suggest that loss of normal functions of htt contributes to the impaired olfactory function seen in HD patients.

A number of functions have been proposed for htt, which may affect brain formation and patterning contributing to a deficiency in anterior neural plate formation. Such functions include promotion of cell survival, differentiation and formation of progenitor cells. Neurotrophins, such as BDNF, are important in mammalian neurons for survival and differentiation. Htt is known to play an important role in regulating the production of BDNF (7–9) and in the transport of BDNF along microtubules (10). Adding exogenous recombinant BDNF to the embryo medium was able to rescue partially the number of lateral line neuromasts toward wild-type levels, suggesting that alteration in the production or supply of BDNF is responsible in part for the loss of lateral line neuromasts. It is currently not clear which step in the formation of lateral line neuromasts is rescued by BDNF—whether in the formation of the anterior neural ectoderm, in its survival or in differentiation of the sensory neurons, a known function of BDNF (62). The significant, yet incomplete, rescue of neuromast number upon addition of BDNF to *hd*MO1 embryos suggests that other distinct (still to be identified) htt interacting pathways may play a role in neuromast development.

A role for htt in brain development is suggested by the high level of htt expression in the brain early in development; however, its precise function at this stage is not clear. Htt has a known important role in neuronal survival, and has been shown to be required for the formation or survival of neurons in specific regions of the brain. A conditional knockout system in mouse has previously shown that htt is required for survival of neurons within the postnatal forebrain (63). More specifically, $Hdh^{-/-}$ ES cells injected into a wild-type blastocyst showed that htt expression was required for neuronal survival within the striatum, cortex, hippocampus and Purkinje cells of the cerebellum (13). These results are complementary to that seen in our zebrafish model of morpholino-induced htt knockdown, highlighting a role for htt in formation or survival of anterior neural tissues.

A search of the literature did not reveal any report of a mutant or morphant zebrafish exhibiting the same constellation of phenotypes brought about by reduction in htt. Therefore, the identity of other participants in these pathways that might be revealed by such mutants awaits more thorough mutation analysis of zebrafish.

In summary, the data presented here demonstrates a role for htt in the formation of the anterior most region of the neural plate using a zebrafish model system of htt knockdown. The advantages of this system enable analysis of htt function at the earliest stages of development, a difficult task in mouse *Hdh* knockout models. Our data show that despite the homogeneous expression of htt in the brain, htt functions specifically within the forebrain to enable formation of precursors of the telencephlon and pre-placodal cells. The downstream effect of this includes loss of placode-derived tissue including olfactory and lateral line sensory neurons, and reduction in telencephalic tissue. The observed sensory neuron requirement for htt in the zebrafish htt depletion model described here is consistent with the observation that HD patients show impaired olfactory function (64–69). This suggests that the loss of normal function of htt contributes to at least some of the symptoms of HD pathology. We have also demonstrated that the htt-dependant reduction in peripheral sensory

Table 2. Primers used for quantative PCR

Gene	Upstream primer (5′ to 3′)	Downstream primer (5′ to 3′)	Product (bp)
dlx3b	GAGGGCTGAGAACACGAACC	TCACCATTCTAATGACCGCT	51
ef1a	CCAACTTCAACGCTCAGGTCA	CAAACTTGCAGGCGATGTGA	105
emx3	GATATCTGGGACACCGGTTTCA	AGCAGGTTTTCAGGGCTACTGT	52
ntl	CACACCACAAACACTACCTCCAAC	TGACCACAGACTTGGGTACTGACT	51
zOMP	GAACCCACCGGACTCTTCTG	TTGGCCAGCTCTGCTATCCT	101
otx2	CCCTCCGTTGGATACCCAGT	TCGTCTCTGCTTTCGAGGAGTC	51
six1	CTACCACACAAGTGAGCAACTGG	AGCGCCCGTGTTGTTGTT	99
val	CAGCTTGTGACCATGTCCGT	TGAAGCCCCGCAGGTGT	52

All primers span introns where possible (exceptions are *zOMP* and *val*).

neurons is rescued partially by BDNF, further highlighting the important developmental role for htt in regulation of BDNF signaling, and the likely participation of BDNF in HD pathology.

MATERIALS AND METHODS

Zebrafish maintenance and staging

Zebrafish were maintained at 28.5°C under standard conditions as described (70). Embryo medium (71) was used to develop fish for all experiments. Developmental stages were determined by using both timing (hours post fertilization, hpf) and morphological features according to Kimmel *et al*. (71). For *in situ* hybridization analysis after 20 hpf, embryos were raised in 40 μM 1-phenyl-2-thiourea (PTU) from gastrula stage (5.5 hpf) to inhibit pigment formation.

Morpholino design

All morpholinos (MOs) used were designed and synthesized by Gene-Tools, LLC Ore and were of the same antisense sequence as described previously (18). *hd*MO1, *hd*MO2, *c*MO and *mc*MO1 morpholinos were prepared and injected in the manner described in ref. (18).

Acridine orange staining

Apoptosis in whole embryos was assessed by staining with the vital dye, acridine orange (AO; Sigma-Aldrich) (72). The acridine orange protocol was adapted from Li and Dowling (73). A stock solution was made up to 1 mg/ml in water. Embryos were dechorionated and placed in 1/1000 dilution of the acridine orange stock solution in embryo medium for 30 min. After washing in embryo medium, the embryos were placed into tricaine anesthetic solution (3-amino benzoic acid ethyl ester; Sigma-Aldrich) (70) and viewed immediately using a green fluorescence filter.

Alcian blue

Alcian blue cartilage stain was used to visualize the structure of the craniofacial skeleton of zebrafish. Five- to 8-day-old larvae were fixed in 4% formaldehyde in 1 × phosphate buffered saline (PBS) overnight at 4°C. Embryos were bleached in 0.5 ml 30% hydrogen peroxide for about 2 h. Twenty-five microlitres of 2 M potassium hydroxide was added to enhance the bleaching process. When eyes appeared sufficiently translucent, embryos were stained overnight in a filtered alcian blue solution (1% concentrated hydrochloric acid, 70% ethanol, 0.1% alcian blue (AnaSpec)). Embryos were cleared in acidic ethanol (5% concentrated hydrochloric acid, 70% ethanol) for 4 h, rehydrated in a graded ethanol series (50%, 25% then PBS), then stored in 80% glycerol at −20°C. Craniofacial cartilage was visualized under a Zeiss Axiophot light microscope and photographed using a 10× objective.

DiI staining

DiI was used to label mature olfactory sensory neurons in live zebrafish embryos (25). DiIC18(3) powder (Invitrogen) was made up to a 5% stock solution in dimethylformamide (DMF). To stain the embryos, 1 μl of DiI stock was added to 5 μl DMF and 4 μl 70% glycerol. The 10 μl working stock of DiI solution was added to 96 hpf zebrafish embryos in 4 ml of embryo medium for 15 min. For viewing, fish were anesthetized in tricaine then mounted in 3% methylcellulose with tricaine. DiI stained olfactory receptor neurons were initially viewed on a dissecting microscope using a rhodamine cube or filter suitable for 550 nm emission −565 nm excitation. Images were captured on a Leica SP5 spectral scanning confocal microscope.

DASPEI staining

DASPEI specifically stains hair cells within lateral line neuromasts (27) of live zebrafish embryos. The staining procedure was carried out as described in ref. (74). One hundred and twenty hours post fertilization live zebrafish embryos were immersed in 1 mM DASPEI in embryo medium for 5 min (supernatant only). The embryos were then rinsed thoroughly in embryo medium before anesthetizing and viewing as described above for DiI. For quantitation, presence or absence of each lateral line neuromast was recorded with reference to the previously described pattern along the lateral side of the embryo (28). Statistical analysis was performed using a Student's *t*-test.

For BDNF rescue experiments, human recombinant BDNF (100 ng/ml; Millipore) was dissolved in water and added to the embryo medium 10 h after morpholino injection. Embryo medium with or without BDNF was replaced with

fresh medium every 24 h. Each experiment was carried out on three separate occasions by a blinded investigator. Seventeen nanogram hdMO1 was injected per embryo.

Whole-mount *in situ* hybridization

In situ hybridization was carried out according to the protocols published by Jowett (75) with minor changes, described as follows. To allow chromogenic detection, alkaline phosphatase conjugated antibody was added at 1:4000 dilution in PBS with 0.1% Tween-20 and 1% BSA for 1 h at 4°C. For two color *in situ* hybridization, NBT/BCIP was used to detect the first (and weakest) probe, prior to detection of the second probe with Vector red. Digoxygenin and fluorescein-labelled antisense probes were synthesized from cDNAs of *krox 20* (64), *gsc* (65), *otx2* (66), *six1* (35), *ntl* (44), *dlx2* (67), *dlx3b* (67), *col2a1* (68), *sox32* (69), *val* (76) and *hoxd4a* (77).

Quantitative PCR

Total RNA was extracted from zebrafish embryos (~30 embryos per sample) and quantitative PCR carried out as described in ref. (18) on an ABI 7000 sequence detection system (Applied Biosciences), where possible primers were designed to span an intron. Exceptions were the genes *zOMP* and *val*. The relative standard curve method was used for quantification (as described by the manufacturer) to generate raw values representing arbitrary units of RNA transcript. Each experiment was performed on three independent occasions except for *val*, which was performed twice. In every experiment, each embryo sample was run in triplicate. The experimental gene value was then normalized to the average *ef1-a* value for that sample. Statistical analyses on normalized data were performed using ANOVA and Student's *t*-tests. Raw *P*-values were adjusted using the false discovery rate method. All primers used are shown in Table 2.

ACKNOWLEDGEMENTS

We wish to thank the members of the Richards lab as well as S. Pederson, who have read drafts of this manuscript and made valuable contributions. We also acknowledge S. Wells and M. Newman for technical assistance with embryo injections and scoring of embryos.

Conflict of Interest statement. None declared.

FUNDING

This work was supported in part by Australian Research Council (ARC) funding to the ARC Special Research Centre for the Molecular Genetics of Development (MGD). Funding to pay the Open Access publication charges for this article was provided by CMGD.

REFERENCES

1. Martin, J.B. and Gusella, J.F. (1986) Huntington's disease. Pathogenesis and management. *N. Engl. J. Med.*, **315**, 1267–1276.
2. HDCRG. (1993) A novel gene containing a trinucleotide repeat that is expanded and unstable on Huntington's disease chromosomes. The Huntington's Disease Collaborative Research Group. *Cell*, **72**, 971–983.
3. Graveland, G.A., Williams, R.S. and DiFiglia, M. (1985) Evidence for degenerative and regenerative changes in neostriatal spiny neurons in Huntington's disease. *Science*, **227**, 770–773.
4. Vonsattel, J.P., Myers, R.H., Stevens, T.J., Ferrante, R.J., Bird, E.D. and Richardson, E.P. Jr (1985) Neuropathological classification of Huntington's disease. *J. Neuropathol. Exp. Neurol.*, **44**, 559–577.
5. Gusella, J.F. and MacDonald, M.E. (2000) Molecular genetics: unmasking polyglutamine triggers in neurodegenerative disease. *Nat. Rev. Neurosci.*, **1**, 109–115.
6. Imarisio, S., Carmichael, J., Korolchuk, V., Chen, C.W., Saiki, S., Rose, C., Krishna, G., Davies, J.E., Ttofi, E., Underwood, B.R. *et al.* (2008) Huntington's disease: from pathology and genetics to potential therapies. *Biochem. J.*, **412**, 191–209.
7. Hodgson, J.G., Agopyan, N., Gutekunst, C.A., Leavitt, B.R., LePiane, F., Singaraja, R., Smith, D.J., Bissada, N., McCutcheon, K., Nasir, J. *et al.* (1999) A YAC mouse model for Huntington's disease with full-length mutant huntingtin, cytoplasmic toxicity, and selective striatal neurodegeneration. *Neuron*, **23**, 181–192.
8. Zuccato, C., Ciammola, A., Rigamonti, D., Leavitt, B.R., Goffredo, D., Conti, L., MacDonald, M.E., Friedlander, R.M., Silani, V., Hayden, M.R. *et al.* (2001) Loss of huntingtin-mediated BDNF gene transcription in Huntington's disease. *Science*, **293**, 493–498.
9. Zuccato, C., Tartari, M., Crotti, A., Goffredo, D., Valenza, M., Conti, L., Cataudella, T., Leavitt, B.R., Hayden, M.R., Timmusk, T. *et al.* (2003) Huntingtin interacts with REST/NRSF to modulate the transcription of NRSE-controlled neuronal genes. *Nat. Genet.*, **35**, 76–83.
10. Gauthier, L.R., Charrin, B.C., Borrell-Pages, M., Dompierre, J.P., Rangone, H., Cordelieres, F.P., De Mey, J., MacDonald, M.E., Lessmann, V., Humbert, S. *et al.* (2004) Huntingtin controls neurotrophic support and survival of neurons by enhancing BDNF vesicular transport along microtubules. *Cell*, **118**, 127–138.
11. Caviston, J.P. and Holzbaur, E.L. (2009) Huntingtin as an essential integrator of intracellular vesicular trafficking. *Trends Cell Biol.*, **19**, 147–155.
12. Duyao, M.P., Auerbach, A.B., Ryan, A., Persichetti, F., Barnes, G.T., McNeil, S.M., Ge, P., Vonsattel, J.P., Gusella, J.F., Joyner, A.L. *et al.* (1995) Inactivation of the mouse Huntington's disease gene homolog Hdh. *Science*, **269**, 407–410.
13. Reiner, A., Del Mar, N., Meade, C.A., Yang, H., Dragatsis, I., Zeitlin, S. and Goldowitz, D. (2001) Neurons lacking huntingtin differentially colonize brain and survive in chimeric mice. *J. Neurosci.*, **21**, 7608–7619.
14. White, J.K., Auerbach, W., Duyao, M.P., Vonsattel, J.P., Gusella, J.F., Joyner, A.L. and MacDonald, M.E. (1997) Huntingtin is required for neurogenesis and is not impaired by the Huntington's disease CAG expansion. *Nat. Genet.*, **17**, 404–410.
15. Woda, J.M., Calzonetti, T., Hilditch-Maguire, P., Duyao, M.P., Conlon, R.A. and MacDonald, M.E. (2005) Inactivation of the Huntington's disease gene (Hdh) impairs anterior streak formation and early patterning of the mouse embryo. *BMC Dev. Biol.*, **5**, 17–29.
16. Zeitlin, S., Liu, J.P., Chapman, D.L., Papaioannou, V.E. and Efstratiadis, A. (1995) Increased apoptosis and early embryonic lethality in mice nullizygous for the Huntington's disease gene homologue. *Nat. Genet.*, **11**, 155–163.
17. Nasir, J., Floresco, S.B., O'Kusky, J.R., Diewert, V.M., Richman, J.M., Zeisler, J., Borowski, A., Marth, J.D., Phillips, A.G. and Hayden, M.R. (1995) Targeted disruption of the Huntington's disease gene results in embryonic lethality and behavioral and morphological changes in heterozygotes. *Cell*, **81**, 811–823.
18. Lumsden, A.L., Henshall, T.L., Dayan, S., Lardelli, M.T. and Richards, R.I. (2007) Huntingtin-deficient zebrafish exhibit defects in iron utilization and development. *Hum. Mol. Genet.*, **16**, 1905–1920.
19. Diekmann, H., Anichtchik, O., Fleming, A., Futter, M., Goldsmith, P., Roach, A. and Rubinsztein, D.C. (2009) Decreased BDNF levels are a major contributor to the embryonic phenotype of huntingtin knockdown zebrafish. *J. Neurosci.*, **29**, 1343–1349.
20. Rigamonti, D., Bauer, J.H., De-Fraja, C., Conti, L., Sipione, S., Sciorati, C., Clementi, E., Hackam, A., Hayden, M.R., Li, Y. *et al.* (2000) Wild-type huntingtin protects from apoptosis upstream of caspase-3. *J. Neurosci.*, **20**, 3705–3713.

21. Futter, M., Diekmann, H., Schoenmakers, E., Sadiq, O., Chatterjee, K. and Rubinsztein, D.C. (2009) Wild-type but not mutant huntingtin modulates the transcriptional activity of liver X receptors. *J. Med. Genet.*, **46**, 438–446.
22. Cole, L.K. and Ross, L.S. (2001) Apoptosis in the developing zebrafish embryo. *Dev. Biol.*, **240**, 123–142.
23. Farbman, A.I. (1994) Developmental biology of olfactory sensory neurons. *Semin. Cell Biol.*, **5**, 3–10.
24. Williams, J.A. and Holder, N. (2000) Cell turnover in neuromasts of zebrafish larvae. *Heart Res.*, **143**, 171–181.
25. Whitlock, K.E. and Westerfield, M. (1998) A transient population of neurons pioneers the olfactory pathway in the zebrafish. *J. Neurosci.*, **18**, 8919–8927.
26. Celik, A., Fuss, S.H. and Korsching, S.I. (2002) Selective targeting of zebrafish olfactory receptor neurons by the endogenous OMP promoter. *Eur. J. Neurosci.*, **15**, 798–806.
27. Collazo, A., Fraser, S.E. and Mabee, P.M. (1994) A dual embryonic origin for vertebrate mechanoreceptors. *Science*, **264**, 426–430.
28. Harris, J.A., Cheng, A.G., Cunningham, L.L., MacDonald, G., Raible, D.W. and Rubel, E.W. (2003) Neomycin-induced hair cell death and rapid regeneration in the lateral line of zebrafish (Danio rerio). *J. Assoc. Res. Otolaryngol.*, **4**, 219–234.
29. Baker, C.V. and Bronner-Fraser, M. (2001) Vertebrate cranial placodes I. Embryonic induction. *Dev. Biol.*, **232**, 1–61.
30. Schlosser, G. (2002) Development and evolution of lateral line placodes in amphibians I. Development. *Zoology (Jena)*, **105**, 119–146.
31. Schlosser, G. (2005) Evolutionary origins of vertebrate placodes: insights from developmental studies and from comparisons with other deuterostomes. *J. Exp. Zoolog. B. Mol. Dev. Evol.*, **304**, 347–399.
32. Schlosser, G. (2006) Induction and specification of cranial placodes. *Dev. Biol.*, **294**, 303–351.
33. Streit, A. (2004) Early development of the cranial sensory nervous system: from a common field to individual placodes. *Dev. Biol.*, **276**, 1–15.
34. Brugmann, S.A. and Moody, S.A. (2005) Induction and specification of the vertebrate ectodermal placodes: precursors of the cranial sensory organs. *Biol. Cell*, **97**, 303–319.
35. Bessarab, D.A., Chong, S.W. and Korzh, V. (2004) Expression of zebrafish six1 during sensory organ development and myogenesis. *Dev. Dyn.*, **230**, 781–786.
36. Whitlock, K.E. and Westerfield, M. (2000) The olfactory placodes of the zebrafish form by convergence of cellular fields at the edge of the neural plate. *Development*, **127**, 3645–3653.
37. Dutta, S., Dietrich, J.E., Aspock, G., Burdine, R.D., Schier, A., Westerfield, M. and Varga, Z.M. (2005) pitx3 defines an equivalence domain for lens and anterior pituitary placode. *Development*, **132**, 1579–1590.
38. Kozlowski, D.J., Murakami, T., Ho, R.K. and Weinberg, E.S. (1997) Regional cell movement and tissue patterning in the zebrafish embryo revealed by fate mapping with caged fluorescein. *Biochem. Cell Biol.*, **75**, 551–562.
39. Toro, S. and Varga, Z.M. (2007) Equivalent progenitor cells in the zebrafish anterior preplacodal field give rise to adenohypophysis, lens, and olfactory placodes. *Semin Cell Dev. Biol.*, **18**, 534–542.
40. Simeone, A., Gulisano, M., Acampora, D., Stornaiuolo, A., Rambaldi, M. and Boncinelli, E. (1992) Two vertebrate homeobox genes related to the Drosophila empty spiracles gene are expressed in the embryonic cerebral cortex. *EMBO J.*, **11**, 2541–2550.
41. Morita, T., Nitta, H., Kiyama, Y., Mori, H. and Mishina, M. (1995) Differential expression of two zebrafish emx homeoprotein mRNAs in the developing brain. *Neurosci. Lett.*, **198**, 131–134.
42. Kawahara, A. and Dawid, I.B. (2002) Developmental expression of zebrafish emx1 during early embryogenesis. *Gene Expr. Patterns*, **2**, 201–206.
43. Solnica-Krezel, L. (2005) Conserved patterns of cell movements during vertebrate gastrulation. *Curr. Biol.*, **15**, R213–R228.
44. Schulte-Merker, S., Ho, R.K., Herrmann, B.G. and Nusslein-Volhard, C. (1992) The protein product of the zebrafish homologue of the mouse T gene is expressed in nuclei of the germ ring and the notochord of the early embryo. *Development*, **116**, 1021–1032.
45. Kanki, J.P. and Ho, R.K. (1997) The development of the posterior body in zebrafish. *Development*, **124**, 881–893.
46. Agathon, A., Thisse, C. and Thisse, B. (2003) The molecular nature of the zebrafish tail organizer. *Nature*, **424**, 448–452.
47. Essner, J.J., Amack, J.D., Nyholm, M.K., Harris, E.B. and Yost, H.J. (2005) Kupffer's vesicle is a ciliated organ of asymmetry in the zebrafish embryo that initiates left-right development of the brain, heart and gut. *Development*, **132**, 1247–1260.
48. Thomas, P. and Beddington, R. (1996) Anterior primitive endoderm may be responsible for patterning the anterior neural plate in the mouse embryo. *Curr. Biol.*, **6**, 1487–1496.
49. Brewster, R. and Dahmane, N. (1999) Getting a-head of the organizer: anterior-posterior patterning of the forebrain. *Bioessays*, **21**, 631–636.
50. Thisse, C., Thisse, B., Halpern, M.E. and Postlethwait, J.H. (1994) Goosecoid expression in neurectoderm and mesendoderm is disrupted in zebrafish cyclops gastrulas. *Dev. Biol.*, **164**, 420–429.
51. Ahrens, K. and Schlosser, G. (2005) Tissues and signals involved in the induction of placodal Six1 expression in Xenopus laevis. *Dev. Biol.*, **288**, 40–59.
52. Gunawardena, S., Her, L.S., Brusch, R.G., Laymon, R.A., Niesman, I.R., Gordesky-Gold, B., Sintasath, L., Bonini, N.M. and Goldstein, L.S. (2003) Disruption of axonal transport by loss of huntingtin or expression of pathogenic polyQ proteins in Drosophila. *Neuron*, **40**, 25–40.
53. Helmlinger, D., Yvert, G., Picaud, S., Merienne, K., Sahel, J., Mandel, J.L. and Devys, D. (2002) Progressive retinal degeneration and dysfunction in R6 Huntington's disease mice. *Hum. Mol. Genet.*, **11**, 3351–3359.
54. Petrasch-Parwez, E., Habbes, H.W., Weickert, S., Lobbecke-Schumacher, M., Striedinger, K., Wieczorek, S., Dermietzel, R. and Epplen, J.T. (2004) Fine-structural analysis and connexin expression in the retina of a transgenic model of Huntington's disease. *J. Comp. Neurol.*, **479**, 181–197.
55. Petrasch-Parwez, E., Saft, C., Schlichting, A., Andrich, J., Napirei, M., Arning, L., Wieczorek, S., Dermietzel, R. and Epplen, J.T. (2005) Is the retina affected in Huntington disease? *Acta Neuropathol. (Berl.)*, **110**, 523–525.
56. Hamilton, J.M., Murphy, C. and Paulsen, J.S. (1999) Odor detection, learning, and memory in Huntington's disease. *J. Int. Neuropsychol. Soc.*, **5**, 609–615.
57. Moberg, P.J. and Doty, R.L. (1997) Olfactory function in Huntington's disease patients and at-risk offspring. *Int. J. Neurosci.*, **89**, 133–139.
58. Nordin, S., Paulsen, J.S. and Murphy, C. (1995) Sensory- and memory-mediated olfactory dysfunction in Huntington's disease. *J. Int. Neuropsychol. Soc.*, **1**, 281–290.
59. Pirogovsky, E., Gilbert, P.E., Jacobson, M., Peavy, G., Wetter, S., Goldstein, J., Corey-Bloom, J. and Murphy, C. (2007) Impairments in source memory for olfactory and visual stimuli in preclinical and clinical stages of Huntington's disease. *J. Clin. Exp. Neuropsychol.*, **29**, 395–404.
60. Bylsma, F.W., Moberg, P.J., Doty, R.L. and Brandt, J. (1997) Odor identification in Huntington's disease patients and asymptomatic gene carriers. *J. Neuropsychiatry Clin. Neurosci.*, **9**, 598–600.
61. Lazic, S.E., Goodman, A.O., Grote, H.E., Blakemore, C., Morton, A.J., Hannan, A.J., van Dellen, A. and Barker, R.A. (2007) Olfactory abnormalities in Huntington's disease: decreased plasticity in the primary olfactory cortex of R6/1 transgenic mice and reduced olfactory discrimination in patients. *Brain Res.*, **1151**, 219–226.
62. Hall, B.K. and Ekanayake, S. (1991) Effects of growth factors on the differentiation of neural crest cells and neural crest cell-derivatives. *Int. J. Dev. Biol.*, **35**, 367–387.
63. Dragatsis, I., Levine, M.S. and Zeitlin, S. (2000) Inactivation of Hdh in the brain and testis results in progressive neurodegeneration and sterility in mice. *Nat. Genet.*, **26**, 300–306.
64. Oxtoby, E. and Jowett, T. (1993) Cloning of the zebrafish krox-20 gene (krx-20) and its expression during hindbrain development. *Nucleic Acids Res.*, **21**, 1087–1095.
65. Schulte-Merker, S., Hammerschmidt, M., Beuchle, D., Cho, K.W., De Robertis, E.M. and Nusslein-Volhard, C. (1994) Expression of zebrafish goosecoid and no tail gene products in wild-type and mutant no tail embryos. *Development*, **120**, 843–852.
66. Mori, H., Miyazaki, Y., Morita, T., Nitta, H. and Mishina, M. (1994) Different spatio-temporal expressions of three otx homeoprotein transcripts during zebrafish embryogenesis. *Brain Res. Mol. Brain Res.*, **27**, 221–231.
67. Akimenko, M.A., Ekker, M., Wegner, J., Lin, W. and Westerfield, M. (1994) Combinatorial expression of three zebrafish genes related to

distal-less: part of a homeobox gene code for the head. *J. Neurosci.*, **14**, 3475–3486.
68. Sachdev, S.W., Dietz, U.H., Oshima, Y., Lang, M.R., Knapik, E.W., Hiraki, Y. and Shukunami, C. (2001) Sequence analysis of zebrafish chondromodulin-1 and expression profile in the notochord and chondrogenic regions during cartilage morphogenesis. *Mech. Dev.*, **105**, 157–162.
69. Kikuchi, Y., Agathon, A., Alexander, J., Thisse, C., Waldron, S., Yelon, D., Thisse, B. and Stainier, D.Y. (2001) Casanova encodes a novel Sox-related protein necessary and sufficient for early endoderm formation in zebrafish. *Genes Dev.*, **15**, 1493–1505.
70. Westerfield, M. (1995) *The Zebrafish Book: A Guide to the Laboratory Use of Zebrafish (Danio rerio)*. University of Oregon Press, Eugene.
71. Kimmel, C.B., Ballard, W.W., Kimmel, S.R., Ullmann, B. and Schilling, T.F. (1995) Stages of embryonic development of the zebrafish. *Dev. Dyn.*, **203**, 253–310.
72. Abrams, J.M., White, K., Fessler, L.I. and Steller, H. (1993) Programmed cell death during Drosophila embryogenesis. *Development*, **117**, 29–43.
73. Li, L. and Dowling, J.E. (1997) A dominant form of inherited retinal degeneration caused by a non-photoreceptor cell-specific mutation. *Proc. Natl Acad. Sci. USA*, **94**, 11645–11650.
74. Whitfield, T.T., Granato, M., van Eeden, F.J., Schach, U., Brand, M., Furutani-Seiki, M., Haffter, P., Hammerschmidt, M., Heisenberg, C.P., Jiang, Y.J. *et al.* (1996) Mutations affecting development of the zebrafish inner ear and lateral line. *Development*, **123**, 241–254.
75. Jowett, T. (2001) Double in situ hybridization techniques in zebrafish. *Methods*, **23**, 345–358.
76. Moens, C.B., Yan, Y.L., Appel, B., Force, A.G. and Kimmel, C.B. (1996) valentino: a zebrafish gene required for normal hindbrain segmentation. *Development*, **122**, 3981–3990.
77. Maves, L. and Kimmel, C.B. (2005) Dynamic and sequential patterning of the zebrafish posterior hindbrain by retinoic acid. *Dev. Biol.*, **285**, 593–605.
78. Tang, R., Dodd, A., Lai, D., McNabb, W.C. and Love, D.R. (2007) Validation of zebrafish (Danio rerio) reference genes for quantitative real-time RT-PCR normalization. *Acta Biochim. Biophys. Sin. (Shanghai)*, **39**, 384–390.